Steel and Composite Structures, *Vol. 25, No. 1 (2017) 117-126*
DOI: https://doi.org/10.12989/scs.2017.25.1.117

Mechanical behavior investigation of steel connections using a modified component method

Shizhe Chen [1,2], Jianrong Pan [*1,2], Hui Yuan [1], Zhuangning Xie [1], Zhan Wang [1,2] and Xian Dong [1]

[1] *School of Civil Engineering and Transportation, South China University of Technology, Guangzhou 510640, China*
[2] *State Key Laboratory of Subtropical Building Science, South China University of Technology, Guangzhou 510640, China*

(*Received November 25, 2016, Revised April 20, 2017, Accepted June 20, 2017*)

Abstract. The component method is an analytical approach for investigating the moment–rotation relationship of steel connections. In this study, the component method was improved from two aspects: (i) load analysis of mechanical model; and (ii) combination of spring elements. An optimized component method with more reasonable component models, spring arrangement position, and boundary conditions was developed using finite element analysis. An experimental testing program in two major-axis and two minor-axis connections under symmetrically loading was carried out to verify this method. The initial rotational stiffness obtained from the optimized component method was consistent with the experimental results. It can be concluded that (i) The coupling stiffness between column and beam flanges significantly affects the effective height of the tensile-column web. (ii) The mechanical properties of the bending components were obtained using an equivalent t-stub model considering the bending capacity of bolts. (iii) Using the optimized mechanical components, the initial rotational stiffness was accurately calculated using the spring system. (iv) The characteristics of moment–rotation relationship for beam to column connections were effectively expressed by the SPRING element analysis model using ABAQUS. The calculations are simpler, and the results are accurate.

Keywords: method optimization; component method; rotational stiffness; spring element; major-axis connection; minor-axis connection

1. Introduction

The component method has been developed and used since the 1970s; it was also used in structure designs as a standard approach by CEN, Eurocode 3 (1998). As specified in Eurocode 3, the beam to column connection is appropriately simulated by a combination of mechanical components, and a mechanical model can be established using linear or nonlinear springs, which are based on the properties of mechanical components. These components, representing the specific part of a connection depending on the type of loading, have different functions for the structural performance. The mechanical effect of a concrete slab on a composite joint has been considered in CEN, Eurocode 4 (2001). The component method, with a clear mechanical concept, has been the main approach for describing the mechanical behavior of steel connections.

A moment–rotation curve is a constitutive relationship curve to express the mechanical behavior of steel connections. The constitutive relationship of a steel connection changes with different construction of connections and external loads. Therefore, the mechanical behavior study of the joint using the component method should consider the type of connection and loading condition. The component method was used in the investigation of extended end-plate connection, including the moment strength (Pitrakkos and Tizani 2015, Simoes and Coelho 2001, Beg *et al*. 2004) and rotational ability (Daniunas and Urbonas 2008) under a static load, mechanical properties at a high temperature (Lin *et al*. 2013, Sulong *et al*. 2010, Wang *et al*. 2007), and cyclic loading (Saravanan *et al*. 2009, Iannone *et al*. 2011). Other types of connections were investigated (Pecce *et al*. 2012). Gil and Bayo (2008a), carried out the experimental and finite element analysis of beam to column composite connections with a flush end-plate connection, revised and improved the unbalanced moment coefficient β, proposed by Eurocode. Lemonis and Gantes (2009) used a combination of the component method and other methods to establish the constitutive curve of an extended end-plate connection and two web and top-seat angle connections. Also, reliable calculations and analysis were carried out for an equivalent T-stub model. Previous studies show that the component method lacks uniform standards for studying the performance of various connections, particularly the minor-axis.

In this study, we adopted the assumption that the section of mechanical component should be plane which was also the basic requirement of the traditional components method. And the component method was revised and improved from two aspects: load analysis of mechanical model, and combination of spring elements. A modified equation (Eq. (9)) was proposed to describe the tensile stiffness of bending components. The components were modeled as

∗Corresponding author, Associate Professor,
E-mail: ctjrpan@scut.edu.cn

http://www.techno-press.org/?journal=scs&subpage=6
ISSN: 1229-9367 (Print), 1598-6233 (Online)

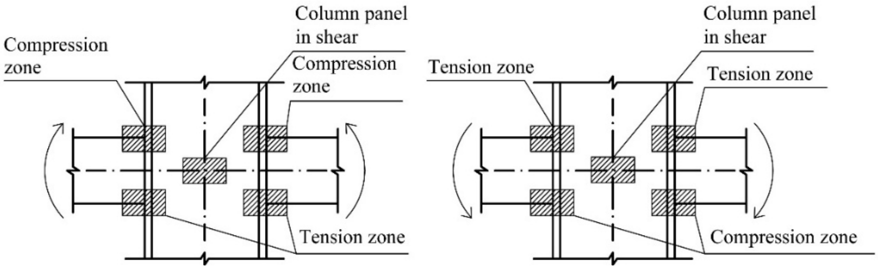

Fig. 1 Analysis of different loading models

spring elements using the ABAQUS software, reasonable boundary conditions were set between springs. In order to verify the spring element component analysis method, experiments of four joints with interior connections were conducted. From the combined experimental and theoretical analysis, the stress components and deformation characteristics of the four groups of interior connections were clearly obtained.

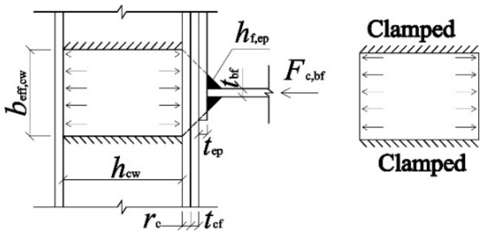

Fig. 2 Simplified model for column web in compression

2. Component analysis method

The moment–rotation relationship shows the constitutive relationship of the beam to column connections. When the structure of beam to column connection or external load changes, its constitutive relationship also changes. This change can be expressed by the initial rotational stiffness of the connection. According to Eurocode, the initial rotational stiffness of the connection can be calculated in two steps: (i) stiffness determination of the basic components; and (ii) initial rotational stiffness calculation of the connection after combining with the basic components. In this study, the steps of the component method were modified as follows: load analysis of connection, development of a mechanical model, establishment of boundary conditions, combination of spring elements.

2.1 Development of mechanical model

The main principle the component method is to simplify the process, converting the complex cross-section into a single load bearing plate or bar. The common mechanical models include compression component, tension component, bending component, and shear component. The theoretical model developed in this paper involves a symmetrical load. Therefore, the shear component will not be discussed.

2.1.1 Tension/compression components

The tension/compression component is a typical plane deformation component. The tension and compression components are essential when the beam to column connection is divided into different components. The tension components include column webs, column flange, high strength bolts, and stiffening ribs. The compression components include the column web and stiffening ribs in the compression zone. The stiffness can be calculated from the cross-sectional dimension and material properties when the high strength bolts and stiffening ribs are treated as independent components.

As shown in Fig. 2, the column web passes through the entire height of the column. Effective width is the key parameter for calculating stiffness when developing the tension/compression model. A study (Li *et al*. 2009) reported that the pressure transferred by the beam flange could spread by 45° between the interlayer plates. The effective width of the compressed column web can be calculated using Eq. (1).

$$K_{\mathrm{cw,c}} = \frac{E_{\mathrm{cw}} t_{\mathrm{cw}} b_{\mathrm{eff,cw}}}{h_{\mathrm{cw}}(1-\nu^2)} \tag{1}$$

$$b_{\mathrm{eff,cw}} = t_{\mathrm{bf}} + 2h_{\mathrm{f,ep}} + 2t_{\mathrm{ep}} + 2(t_{\mathrm{cf}} + r_{\mathrm{c}}) \tag{2}$$

Where υ is the poisson ratio of steel, t_{bf} is the thickness of the beam flange, $h_{f,ep}$ is the effective height of the weld between the steel beam and end-plate, t_{ep} is the end-plate thickness, t_{cf} is the column flange thickness, and r_c is the root radius of the column flange for hot rolled steel section and the effective height of the weld connecting column flange and web for welded steel section (Wang and Chen 2008). The effective width of the tension-column web is affected by the stiffness of beam to column connection and bolt spacing. When the stiffness of a beam to column connection is strong (welding), the effective width of tension zone is distributed by the tension force in column web which is transmitted from the column flange. And, the method of calculating the effective width is the same as compression zone. When the stiffness of a beam to column connection is weak (bolt connection), the tension on the beam flange will be first transferred to the bolt, and then to the column web through the tensile bolt. Therefore, the effective width should be measured through the bolt center after spreading 45° (Li *et al*. 2009). When the bolt spacing is large, the effective width of the column web is not affected by the adjacent bolt, as shown in Fig. 3(a). When the bolt spacing is small, the effective width of the adjacent

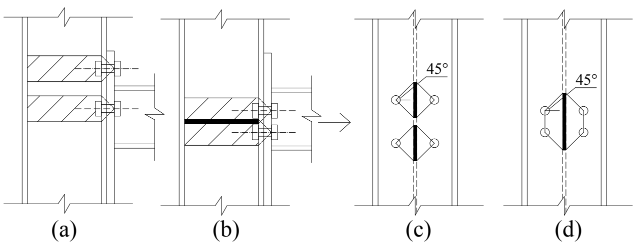

Fig. 3 Effect of bolt pitch on the effective width of tensile-column web

bolt in the column web overlaps to an extent. In the calculation, the overlapped width should be subtracted from the total width. Figs. 3(b), (c), and (d) show the tension diffusion state of the column web in two types of bolt spacing.

The initial tensile stiffness of a T-stub is mostly calculated using the multispan continuous beam method (Wang and Chen 2008). However, the calculation does not consider the effect of the bending rigidity of the bolt. In this study, a partial-clamped constraint state is proposed to consider the bending effect of bolts, as shown in Fig. 5. The overall deformation of T-stub should be divided into Δ_t and Δ_s, where Δ_t is the bending deformation of the flange and bolt. Δ_s is the axial deformation of the preloaded bolts. The initial tensile stiffness of T-stub could be calculated through the overall deformation of Δ_t and Δ_s under unit-load.

The initial tensile stiffness (K_s) of bolt-plate components considering the preloaded force of bolt should be the tangent stiffness under two-thirds of yield load, and Δ_s could be calculated as follows

$$\Delta_{\rm s} = \frac{1/2F}{K_{\rm s}} = \frac{1/2F}{2n\lambda K_{\rm b} / (3\ln\left|\frac{3+3\lambda}{3+\lambda}\right|)} \tag{3}$$

$$\lambda = 5.7 + 2.95 t_{\rm a} / d_{\rm bolt} \tag{4}$$

Where K_b is the tensile stiffness of bolt, n is the number of connecting plates, d_{bolt} is the nominal diameter of bolt, and t_a is the average thickness of both the pieces of the connecting plate.

In order to simplify the calculation, the flange plate was considered from one side of the support to mid-span, and a symmetry constraint was also applied (Fig. 5(c)). Thus, the bending moments are as follows

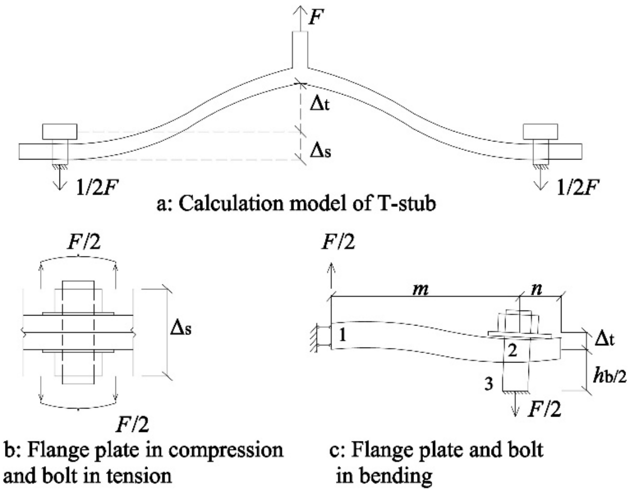

Fig. 5 Calculation diagram of partial-clamped beam

$$M_{12} = \frac{F}{2} \cdot m \cdot \frac{1+2\gamma}{1+4\gamma} \tag{5}$$

$$M_{21} = \frac{F}{2} \cdot m \cdot \frac{2\gamma}{1+4\gamma} \tag{6}$$

$$\gamma = 0.589 \cdot \frac{m}{h_{\rm b/2}} \cdot \frac{d_{\rm bolt}^4}{b_{\rm eff} t_{\rm f}^3} \tag{7}$$

The deformation caused by the bending of the flange plate and bolt can be calculated using the diagrammatic multiplication method (Stamatopoulos and Ermopoulos 2010)

$$\Delta_{\rm t} = \frac{1}{EI} \cdot \frac{l^2}{8} \cdot (\frac{2}{3} M_{12} - \frac{1}{2} M_{21}) \tag{8}$$

Where b_{eff} is the effective width of a T-stub model, and the value of b_{eff} can be referred to reference (Li *et al*. 2009); t_f is the flange thickness of the T-stub model.

The stiffness of T-stub can be calculated using the following equation

$$K_{\rm T\text{-}stub} = \frac{1}{\frac{1}{48} \cdot \frac{l^3}{EI} \cdot \frac{1+\gamma}{1+4\gamma} + \frac{3\ln\left|\frac{3+3\lambda}{3+\lambda}\right|}{2n\lambda K_{\rm b}}} \tag{9}$$

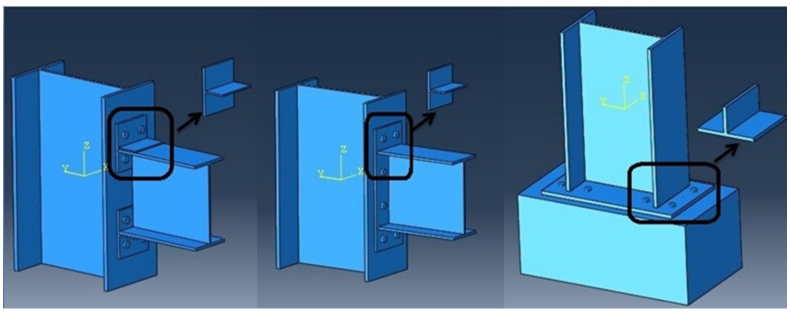

Fig. 4 Identification of tensile T-stubs in various steel joints

Table 1 Tensile stiffness values of T-stub (unit: kN/mm)

Number of specimens	Experiment results	Eq. (9)		EC3($K=\frac{0.9Eb_{\text{eff}}t_f^3}{m^3}$)	
		Calculated results	Deviation	Calculated results	Deviation
T-1	112	148.6	32.68%	173.81	55.19%
T-2	552	503	-8.88%	711.94	28.97%
T-3	77.36	61.7	-20.24%	66.86	-13.57%
T-6	260	195.86	-24.67%	248.64	-4.37%
T-7	438	430.85	-1.63%	412	-5.93%
T-8	164	133.17	-18.8%	155.64	-5.1%
Average deviation			-6.92%		-9.3%

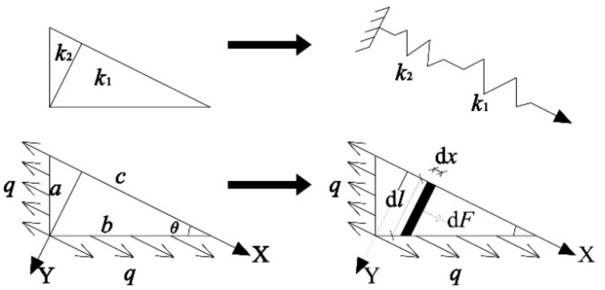

Fig. 6 Mechanical model of stiffener

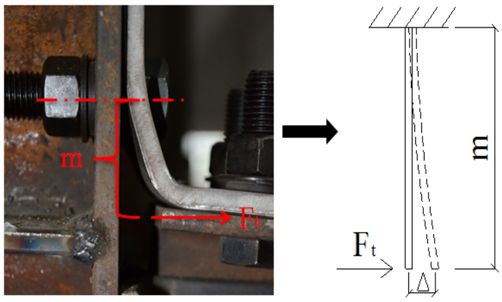

Fig. 7 Mechanical model of top angle

The results calculated by Eq. (9) are acceptable compared with the equation provided by EC3, as shown in Table 1. The T-stub dimensions and the experimental data were referenced from Chen (2015).

2.1.3 Other conventional force components

Fig. 6 shows the stress model of the stiffening rib. Under a bending moment, the stiffening rib can be simplified into a variable section bar. The uniformly distributed load is along the right-angle sides and parallel to the X-axis. The tensile/compressive stiffness of the stiffening rib can be obtained by stiffness integral of the variable cross-sections along the X-axis.

$$K_{\text{stiffener}}=\frac{1}{1/k_1+1/k_2}=\frac{E\cdot t}{\tan\theta+\cot\theta}=\frac{E\cdot t}{a/b+b/a}=\frac{a\cdot b\cdot E\cdot t}{c^2} \tag{10}$$

$$k_1=\frac{F}{\Delta l}=\frac{b\cdot\sin\theta\cdot t\cdot q}{\frac{b\cdot\cos\theta\cdot q}{E}}=E\cdot t\cdot\tan\theta \tag{11}$$

$$k_2=E\cdot t\cdot\cot\theta \tag{12}$$

As shown in Fig. 7, the bending member in top/seat angle connections has no symmetrical bolt constraint, the stress model can be simplified as a cantilever beam supported by a single bolt as follows

$$K_{\text{ep}}=\frac{3EI}{m^3} \tag{13}$$

Where EI is the bending rigidity of the angle, and m is the distance from the center of the bolt to the load end.

2.2 Set of boundary conditions and combination of spring elements

The SPRING element, which can effectively simulate the axial mechanical behavior between two points, was adopted for modeling the mechanical component. Shell elements (S4R) were adopted to simplify the components of the beam. The combination of spring element and shell element could provide more reasonable boundary conditions and spring locations.

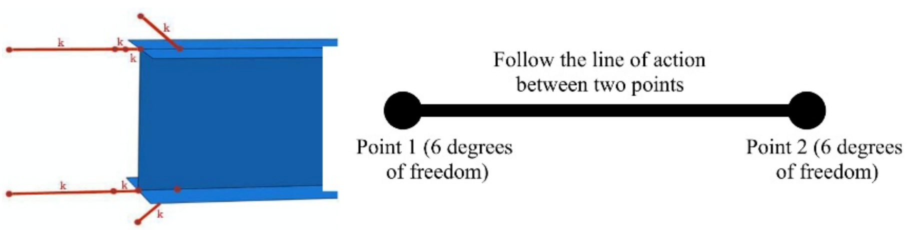

Fig. 8 Spring elements

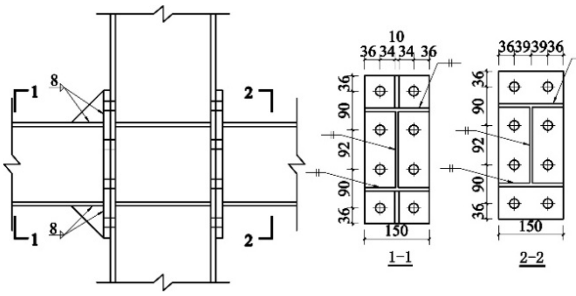

(a) Major-axis extended end-plate connections (TS1)

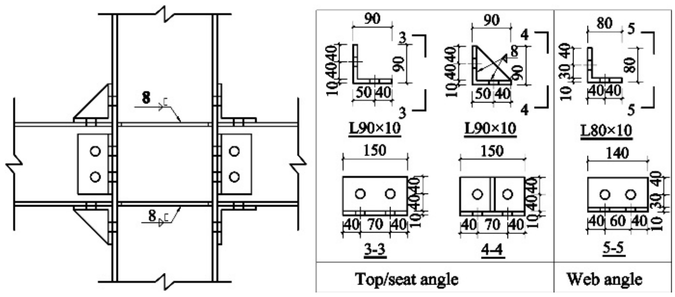

(b) Major-axis top and seat angles with double web angel connection (TS2)

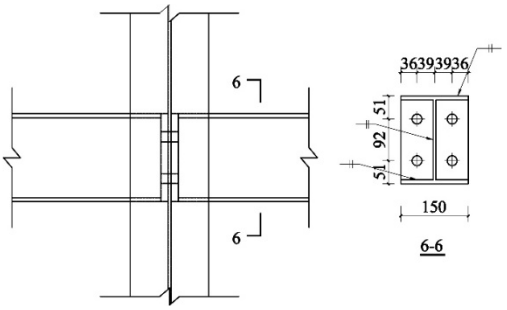

(c) Minor-axis flush end-plate connection (TS3)

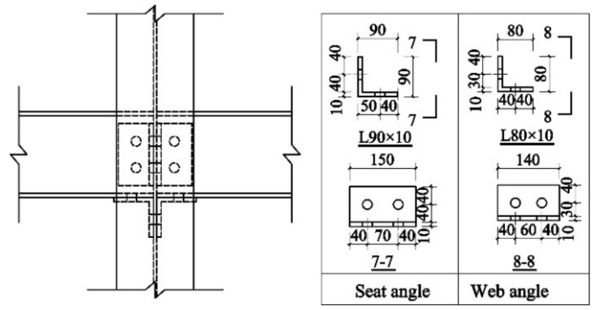

(d) Minor-axis seat angles with double web angel connections (TS4)

Fig. 9 Details of the experimentally tested beam to column connections

3. Experimental study

3.1 Specimen design and test device

To verify the accuracy of the theoretical analysis of the component model, experiments of four joints were carried out with major-axis and minor-axis connections, commonly used in engineering. Symmetrical loading were chosen for more stable loading conditions, and the extraction of mechanical components could be more accurate. The details of the beam to column connection are shown in Fig. 9. According to major-axis connections, stiffening ribs were fixed on the left beam to investigate their contribution to the stiffness of the connection. The steel grade was Q235. All the welds were first-grade weld. The frictional-type high strength bolts used are 10.9 grade. The main parameters of the specimen are shown in Table 2.

The test mainly includes four interior joints under symmetric loading and the material quality testing of the components. The loading devices are shown in Figs. 10-11. The properties of components are listed in Table 3. The bottom of the column was fixed on a rigid foundation plate with four high strength bolts. The top of the column was fixed with an axial-forcing jack, which could move horizon-

Table 2 Main parameters of specimens (unit: mm)

Number of specimens	Column section	Column length	Beam section	Beam length	Bolt diameter	Remarks
TS1	HM244 × 175 × 7 × 11	2000	HM194 × 150 × 6 × 9	1000	20	Major-axis
TS2	HM244 × 175 × 7 × 11	2000	HM194 × 150 × 6× 9	1000	20	Major-axis
TS3	HM244 × 175 × 7 × 11	2000	HM194 × 150 × 6 × 9	1000	20	Minor-axis
TS4	HM244 × 175 × 7 × 11	2000	HM194 × 150 × 6 × 9	1000	20	Minor-axis

Table 3 Material properties of components

Material component	Yield strength f_y (MPa)	Ultimate strength f_u (MPa)	Modulus of elasticity E (GPa)	Elongation $\Delta L/L$ (%)
Stiffening rib	263.5	466.9	204.8	22
Column	262.4	435.3	196	22.7
Angle	253.1	396.6	210	22
End-plate	263.1	445.6	206	17.2

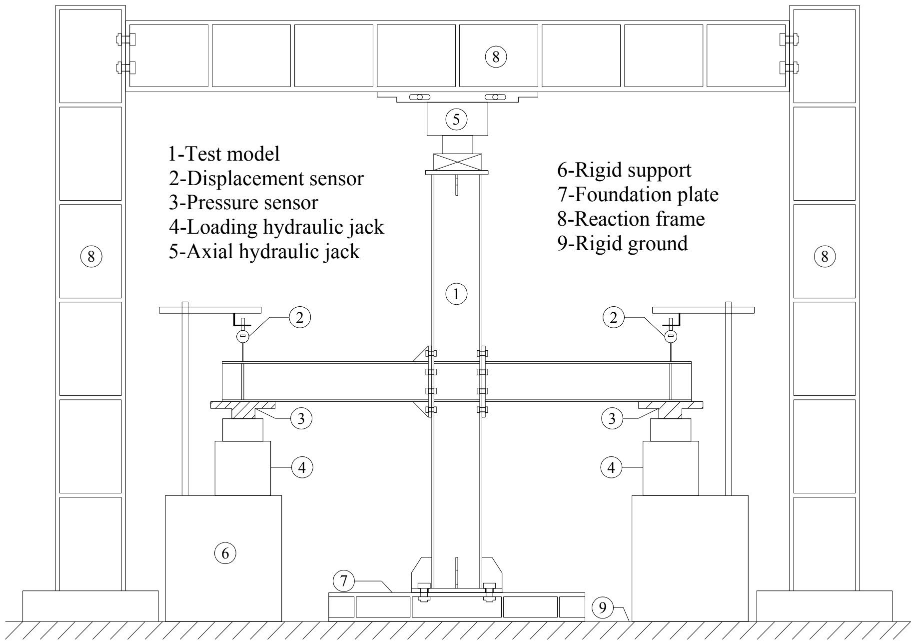

Fig. 10 Testing rig

Fig. 11 Joint of interior column loaded

(a) Elastic stage

(b) Plastic stage

Fig. 12 Moment–rotation relationship of interior connections

tally along the reaction frame. At the ends of the beam, synchronous symmetric loading was applied using a jack. At the same time, the displacement sensor and load sensor were monitored to synchronize the data.

3.2 Test content and bending moment analysis

The main contents include the vertical displacement of the beam, vertical load of the beam end, strain of the connection, and failure mode of the entire connection. Wang and Wang (2012) reported that the displacement of beam end has a nonlinear relationship with rotation angle, as shown in Fig. 12. The displacement of the beam end in the elastic stage consists the joint rotation angle and deflection of the beam itself. In the plastic stage, the effect of beam plastic deformation should be considered.

Therefore, the moment–rotation relationship of the connection was calculated using Eqs. (14) and (15).

$$s = \theta L + ML^2 / (3EI) \quad (14)$$

$$s = \theta L + \theta' L + ML^2 / (3EI) \quad (15)$$

Where s is the vertical displacement of the beam end, θ is the rotation angel of the beam to column connection, θ' is the plastic rotation angel of the beam, M is the moment of the beam end, L is the length of the beam, and EI is the bending rigidity of the beam.

4. Verification using the SPRING element component method

4.1 Component analysis of test joints and combination of spring elements

The loadings of the four testing joints were analyzed by combining theoretical and experimental procedures. Column web in shear in the major-axis connection is a non-ignorable component according to the mechanical behavior analysis of the connection. The mechanical properties provide the tensile stiffness in the tension zone and compressive stiffness in the compression zone. Under the action of a symmetrical load, the effect of the column web can be neglected in the minor-axis connection. In the beam-column connection area, the components with a stiffness ontribution to the entire joint include the bending of column flange, end-plate bending, tension/compression of stiffener, and bending of angle steel. The effective components of the four connections are shown in Fig. 13.

The combined components model of the specimens was developed, and its axial rigidity was calculated, as listed in Table 4. While calculation model of plate components in bending could be transformed as T-stub in tension. The form of spring combination and the specialized boundary conditions are shown in Fig. 14. Each spring is located along the main forced direction of the corresponding component, and the length of springs are according with the actual physical length of the components.

4.2 Comparative analysis of results

The finite element software ABAQUS was used to establish the spring combination model of the beam to column connection. Further, the plate element (S4R) was used to establish the original size of the beam model. The material properties were determined experimentally. The loading condition is exactly the same as the test condition. After the calculations, the bending behavior of the interior joints was evaluated. Fig. 15 shows a comparison between the experimental and theoretical analyzes. The stiffness is zero at the first stage in some experiments because of the

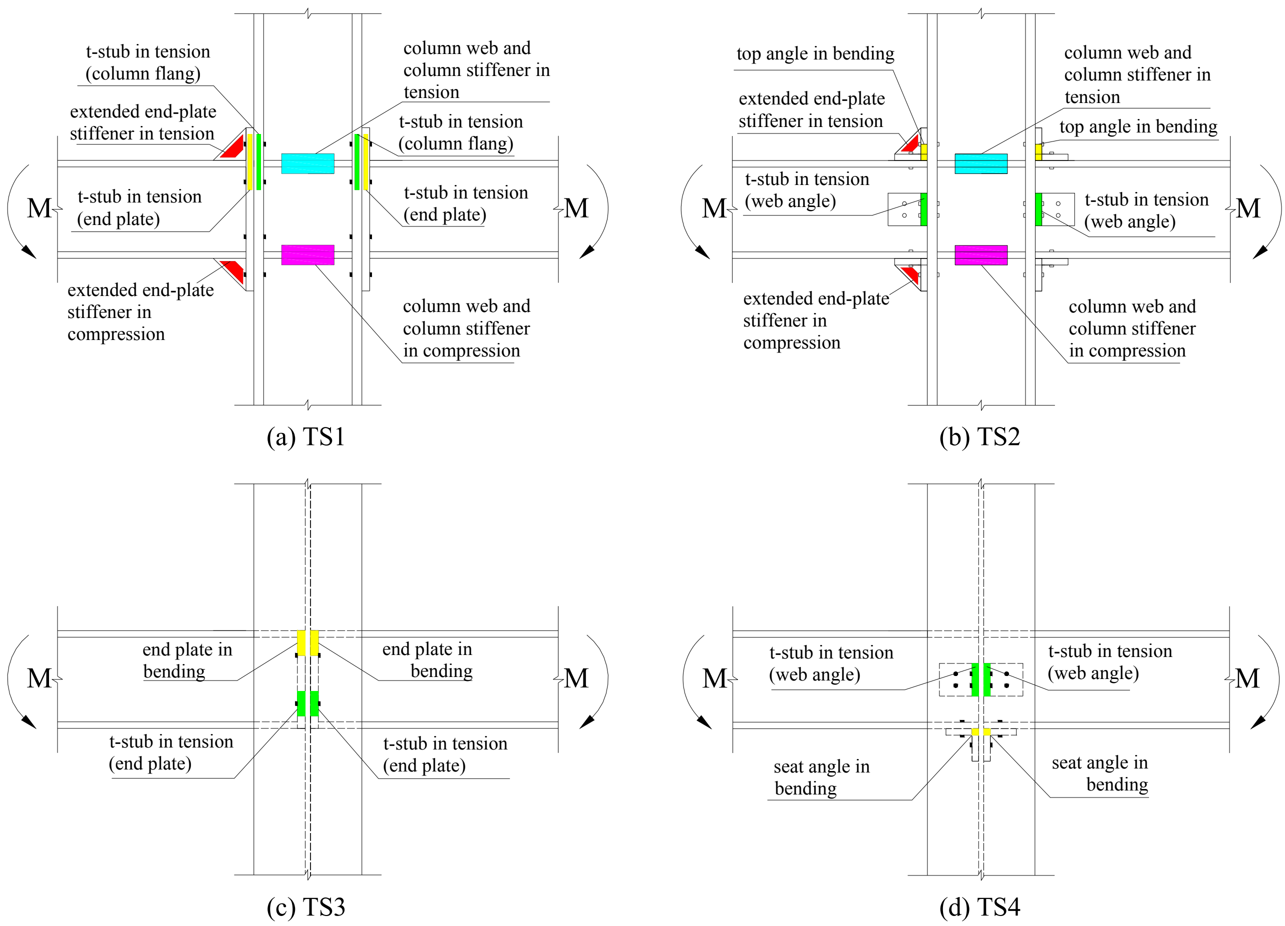

Fig. 13 Loading components of joints

Table 4 Stiffness of components (unit: kN/mm)

Components and numbers	TS1	TS2	TS3	TS4
Column web tension (k1)	1020126	2032876		
Column flange bending (k2)	1728714			
End-plate bending (k3)	2643016		238532	
Stiffener in tension/compression (k4)	1040000	1040000		
Column web compression (k5)	613367	2032876		
Top angle steel bending (k6)		61800		
Web angle steel bending (k7)		427845		386250
Bottom end-plate bending (k8)			2381962	

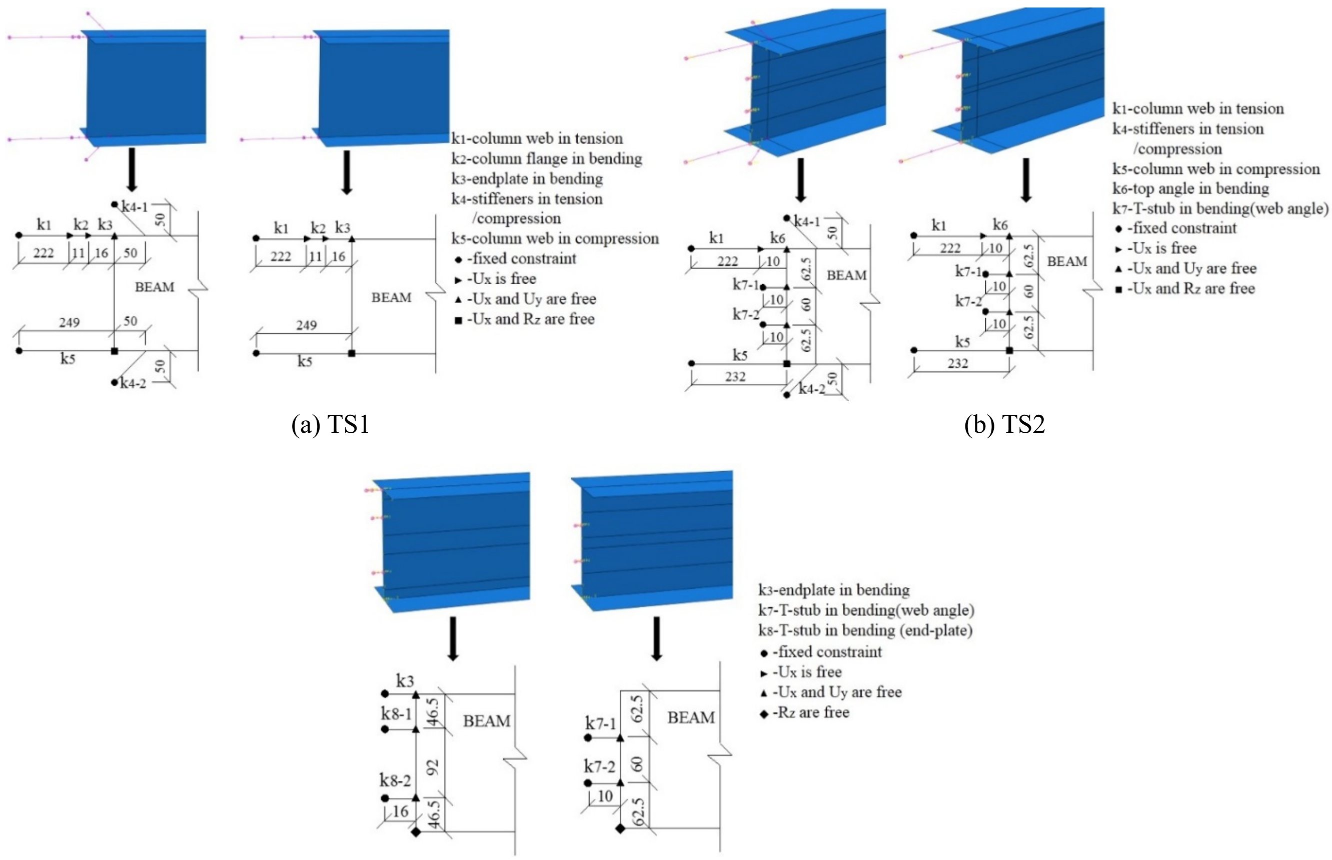

(a) TS1 (b) TS2

(c) TS3 and TS4

Fig. 14 Spring models of four types of connections

Table 5 Initial stiffness values of specimens (unit: kN•m/rad)

Data source	TS1		TS2		TS3	TS4
	Left beam	Right beam	Left beam	Right beam		
Experiment	8947.45	7308.55	6902.2	4500.15	8837.5	3694.5
Spring model	9448	7112.7	7307.6	4353.6	8286.5	3428.6
Deviation	5.6%	2.7%	5.9%	3.3%	6.2%	7.1%

unavoidable virtual displacement at the load-end, however the overall moment-rotation curves of experiments are acceptable compared with the theoretical analyzes. The stiffness data are shown in Table 5.

The combined curves and stiffness data show that the stiffening rib significantly affected the stiffness of the connection. The spring element method based on ABAQUS can effectively simulate the bending performance of the

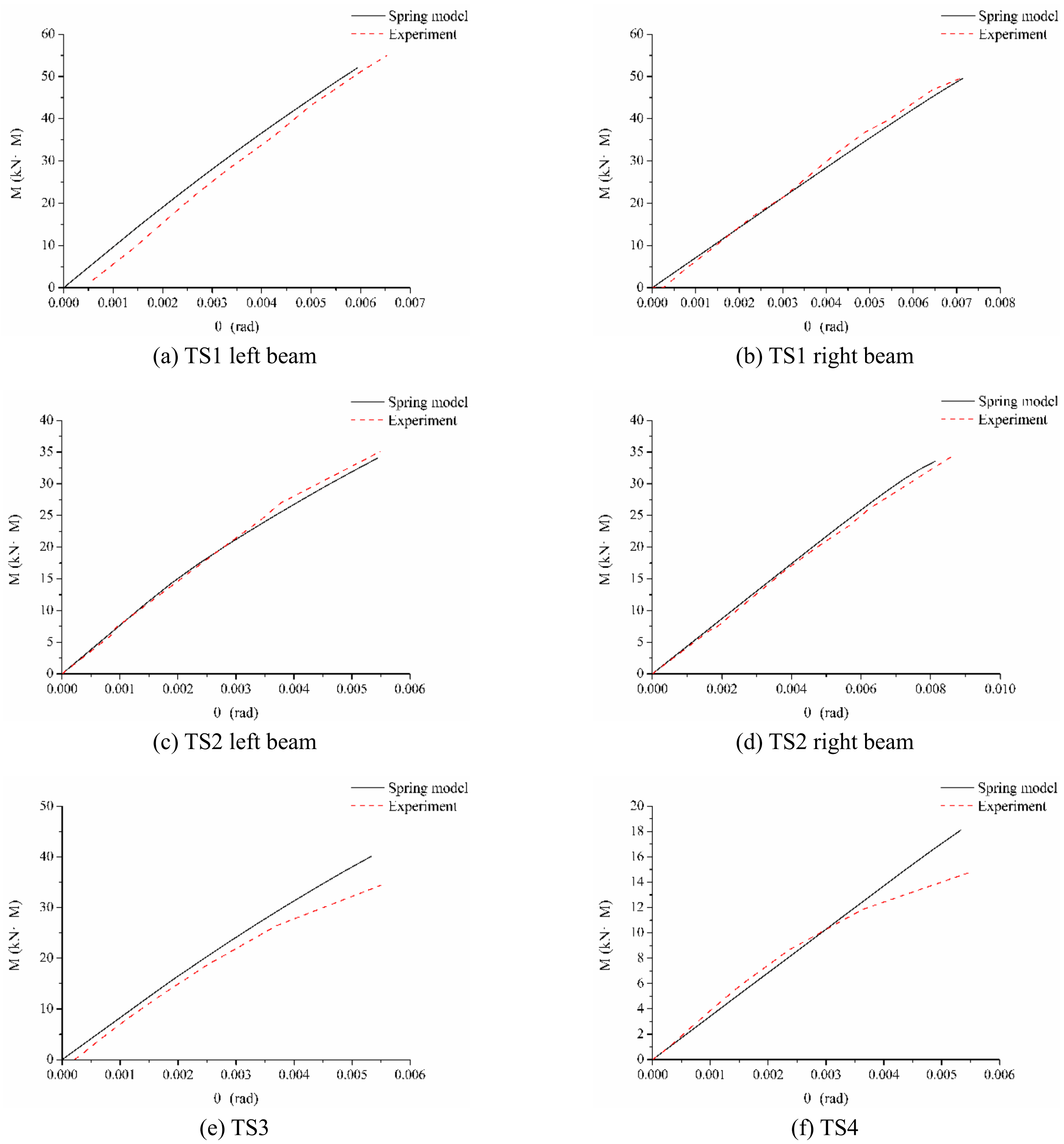

Fig. 15 Moment–rotation curves of FEM analysis and experiments

connection in the elastic stage and provide more accurate initial rotational stiffness. The deviation was bound within 10%. Therefore, the improved component analysis method can be effectively applied to study the constitutive relationship of steel structure joints.

5. Conclusions

According to this study, the following conclusions are drawn:

An equivalent T-stub model considering the bending stiffness of the bolts was proposed to predict the mechanical properties of the bending components. The tensile stiffness equation (Eq. (9)) of T-stub was modified and the results were acceptable compared with the equation provided by EC3.

Using the component method of spring elements, spring layout position and spring boundary conditions are more acceptable with the practical mechanical model which provides more accurate component position and component stiffness. At the same time, the effect of the change in spring position on the geometrical nonlinearity of the entire system can be considered in the calculation. The optimized mechanical model can be efficiently used in the calculation of the initial rotational stiffness of a spring system and the deviation was within 10%.

The spring combination method developed using the finite element software provides the characteristics of moment–rotation relationship of the beam to column connection effectively in the elastic stage. The pre process is more convenient and the calculating is faster compared with the solid modeling based on finite element software. This method has important significance for the rapid prediction of the performance of the beam to column connection.

Acknowledgments

This study was supported by National Natural Science Foundation of China (Grant No. 51378009; 51378219; 51638009), and by State Key Laboratory of Subtropical Building Science of South China University of Technology (Grant No. 2017ZB28, and 2017KD22) and by the Fundamental Research Funds for the Central Universities (Grant No. 2017BQ086; 2017ZD026 and 2017BQ088).

References

Beg, D., Zupancic, E. and Vayas, I. (2004), "On the rotation capacity of moment connections", *J. Constr. Steel Res.*, **60**(3), 601-620.
CEN, Eurocode 3 (1998), Design of steel structures. Part 1.1: General rules and rules for buildings; European Committee for Standardization, Brussels, Belgium.
CEN, Eurocode 4 (2001), Design of composite steel and concrete structures. Part 1.1: General rules and rules for buildings; European Committee for Standardization, Brussels, Belgium.
Chen, S.Z. (2015), "Application of modified and improved component method in the constitutive relation research for steel connections", Ph.D. Dissertation; South China University of Technology, Guangzhou, China.
Daniunas, A. and Urbonas, K. (2008), "Analysis of the steel frames with semi-rigid beam-to-beam and beam-to-column knee joints under bending and axial forces", *Eng. Struct.*, **30**(11), 3114-3118.
Gil, B. and Bayo, E. (2008a), "An alternative design for internal and external semi-rigid composite joints. Part I: Experimental research", *Eng. Struct.*, **30**(1), 218-231.
Gil, B. and Bayo, E. (2008b), "An alternative design for internal and external semi-rigid composite joints. Part II: Finite element modelling and analytical", *Eng. Struct.*, **30**(1), 232-246.
Iannone, F., Latour, M. and Piluso, V. (2011), "Experimental analysis of bolted steel beam-to-column connections: Component identification", *J. Earthq. Eng.*, **15**(2), 214-244.
Lemonis, M.E. and Gantes, C.J. (2009), "Mechanical modeling of the nonlinear response of beam-to-column joints", *J. Constr. Steel Res.*, **65**(4), 879-890.
Li, G.Q., Shi, W.L. and Wang, J.F. (2009), *Design of Steel Frames with Semi-rigid Connections*, China Architecture & Building Press, pp. 70-84.
Lin, S., Huang, Z. and Fan, M. (2013), "Analysis of end-plate connections at elevated temperatures", *Steel Compos. Struct., Int. J.*, **15**(1), 81-101.
Pecce, M., Rossi, F., Bibbo, F.A. and Ceroni, F. (2012), "Experimental behaviour of composite beams subjected to a hogging moment", *Steel Compos. Struct., Int. J.*, **12**(5), 395-412.
Pitrakkos, T, and Tizani, W. (2015), "A component method model for blind-bolts with headed anchors in tension", *Steel Compos. Struct., Int. J.*, **18**(5), 1305-1330.
Saravanan, M., Arul, Jayachandran, S., Marimuthu, V. and Prabha, P. (2009), "Advanced analysis of cyclic behaviour of plane steel frames with semi-rigid connections", *Steel Compos. Struct., Int. J.*, **9**(4), 381-395.
Simoes, D.A. and Coelho, A.M.G. (2001), "A ductility model for steel connections", *J. Constr. Steel Res.*, **57**(1), 45-70.
Stamatopoulos, G.N. and Ermopoulos, J.C. (2010), "Influence of the T-stub flexibility on its strength", *Int. J. Steel Struct.*, **10**(1), 73-79.
Sulong, N.H.R., Elghazouli, A.Y., Izzuddin, B.A. and Ajit, N. (2010), "Modelling of beam-to-column connections at elevated temperature using the component method", *Steel Compos. Struct., Int. J.*, **10**(1), 23-43.
Wang, S.F. and Chen, Y.Y. (2007), "Theoretical model for the initial stiffness of bolted t-stub connection", *Ind. Constr.*, **37**(10), 80-83.
Wang, S.F. and Chen, Y.Y. (2008), "Calculation of initial stiffness of beam-to-column end-plate joint", *Eng. Mech.*, **25**(8), 109-115.
Wang, Z. and Wang, T. (2012), "Experiment and finite element analysis for the end plate minor axis connection of semi-rigid steel frames", *China Civil Eng. J.*, **45**(8), 86-89.
Wang, W.Y., Li, G.Q. and Dong, Y.L. (2007), "Experimental study and spring-component modeling of extended end-plate joints in fire", *J. Constr. Steel Res.*, **63**(8), 1127-1137.

CC